arXiv:astro-ph/9712354v1 31 Dec 1997

Small-Scale Mixing of the Elements

Bruce G. Elmegreen

IBM Research Division, T.J. Watson Research Center, P.O. Box 218, Yorktown Heights, NY 10598 USA, bge@watson.ibm.com

Abstract. The progressive mixing and contamination of interstellar gas by supernovae and other processes following the passage of a spiral density wave is reviewed, with an emphasis on the Solar neighborhood. Regions of star formation should begin their lives with an inhomogeneous mixture of abundances as a result of their chaotic and large-scale formation processes. These inhomogeneities should continue to increase during several generations of star formation until the gas enters the interarm region. Then cloud dispersal by large interarm tidal forces, high rates of shear, and internal star formation should all lead to cloud-to-cloud mixing, while increased ionization, heating, and evaporation should lead to mixing on the atomic level. Gradients in the dispersion of elemental abundances are expected for galaxy disks.

to be published in "Abundance Profiles: Diagnostic Tools for Galaxy History," ed. D. Friedli, M.G. Edmunds, C. Robert, & L. Drissen, ASP Conference Series, 1998.

1. Introduction: The Star-Formation Process

Much of the interstellar gas is hierarchically structured, with relative velocities that increase approximately as the square root of the separation. These and other power law correlations between cloud properties imply that the structure is scale-free, in which case the title of this paper, "small-scale mixing" can actually refer to a wide range of scales. We restrict the discussion, though, to contamination and mixing processes that operate on scales smaller than or equal to one scale height. This includes much of the gas dynamics prior to star formation, essentially all of it during star formation, and some of it after star formation. We also consider only gas processes, and not stellar migration or other stellar mixing processes, even though these stellar processes may dominate the observed star-to-star abundance dispersion at any particular galactic radius. A third restriction is to galaxies like the Milky Way, and in some discussions, to the Solar neighborhood of the Milky Way, because this is the type of region where we know the most about abundance dispersions.

2. Mixing of the ISM Before Star Formation Begins

Most star formation seems to begin on a large scale, comparable to the thickness of the Galaxy disk. In galaxies like ours, which contain strong spiral density

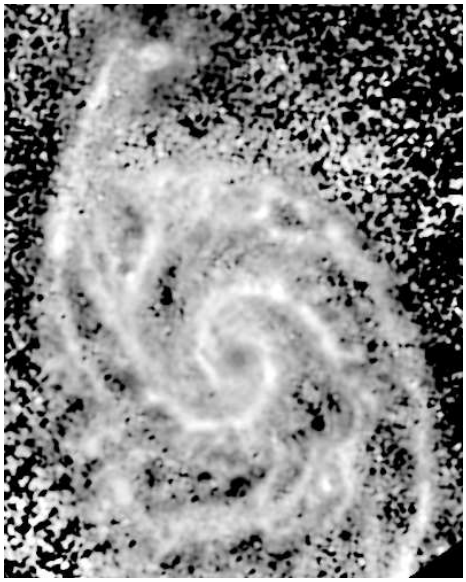

Figure 1. An image of M51 made from the ratio of 15μ emission to B band emission, showing both the warm emitting dust and the cold absorbing dust as bright features. The gas concentrations that lead to star formation in the spiral arms are easily seen at this resolution of 15'. Image from Block et al. (1997).

waves, it begins in the spiral arms in giant gas clouds that typically have a mass of $\sim 10^7$ $M_\odot$. These are observed in atomic gas in many galaxies, such as the Milky Way (Grabelsky et al. 1987; Elmegreen & Elmegreen 1987), M100 (Knapen et al. 1993), and M31 (Lada et al. 1988), and they are observed in molecular gas in other galaxies, such as M51 (Rand & Kulkarni 1990).

Figure 1 shows the gas distribution for M51 made from a combination of dust absorption in the B band and dust emission at 15 μ from ISO (Block et al. 1997). The large knots in the spiral arms, separated by several kiloparsecs, are the main regions of star formation, as shown by Hα and CO. Several giant shells can also be seen in the northern and southern arms in the region of corotation.

Spiral arm gas concentrations like those shown in figure 1 presumably form by the gravitational collapse of density-wave-compressed gas, involving collapse motions along the direction of the arm. The existing theory of this process gives the correct cloud spacing of ~ 3 spiral arm widths, or about 2.5 kpc in galaxies like ours, and it gives the correct cloud mass and a short enough time scale for these clouds to form while the gas is still in the arm (Elmegreen 1994). The formation of such giant clouds is not limited to density wave arms, however, since equally large clouds appear in galaxies with only weak arms (Thornley & Mundy 1997a,b) and in irregular galaxies (Cohen et al. 1988; Hunter 1997). The peculiar conditions in the crest of a strong spiral arm, namely, the high gas density, the low rate of shear, and the low galactic tidal force, make this place highly favored over other sites in galaxies that have spiral waves.

The onset of star formation in spiral arms implies that star-forming clouds begin their lives in violent conditions, possibly inside shock fronts, over a galactic

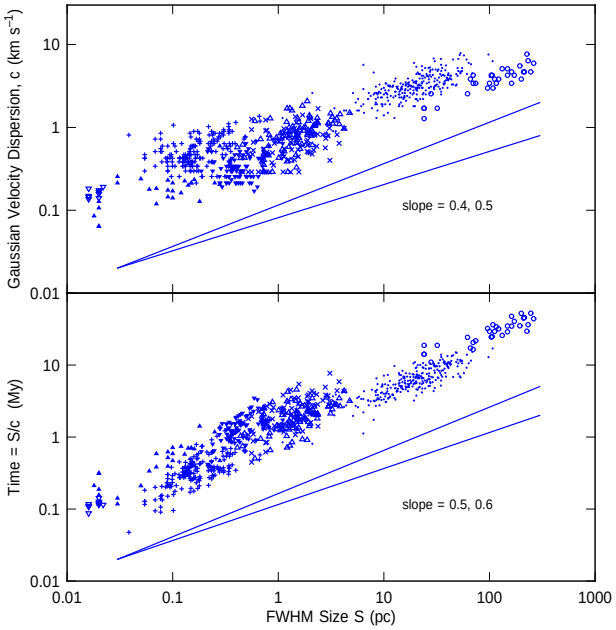

Figure 2. Size and linewidth data from GMC surveys. Symbols are for GMC surveys = *dots*: Solomon et al. (1987), *open circles*: Dame et al. (1986); quiescent clouds = *filled triangles*: Falgarone et al. (1992), *open triangles*: Williams et al. (1994; the Maddalena-Thaddeus cloud), *inverted open triangles*: Lemme et al. (1995; L1498), *inverted filled triangles*: Loren (1989; Ophiuchus), OB associations = *crosses*: Williams et al. (1994; Rosette), *plus signs*: Stutzki & Güsten (1990; M17).

radial range of $\sim$ 1 kpc, considering a typical arm pitch angle of $\sim 15°$. This means that the pre-star-forming gas will be highly turbulent, and it will have a range of metallicities from the background galactic gradient that may be ± 0.05 dex.

The onset of star formation inside such a cloud is relatively quick. It seems to being after a time comparable to the turbulent crossing time, regardless of scale. This time is is $\sim 0.7 S(pc)^{0.5}$ My for scale size S, as determined from the molecular cloud size-linewidth correlation, shown in figure 2. At the top of the figure is the linewidth versus size, and at the bottom is the ratio of size to linewidth, versus size. The *duration* of star formation in a region is also proportional to the local crossing time, perhaps equal to several times this for a wide range of scales (Elmegreen & Efremov 1996). That is, small regions or small clumps form their stars quickly and disperse, while large regions or large clouds take a long time. A schematic diagram of this trend is shown in Figure 3. The correlation between crossing time and size, shown at the bottom of figure 2, is similar to the correlation between duration of star formation and size, shown in figure 3.

A quick onset to star formation in a cloud born under violent and turbulent conditions implies that any non-uniformity of abundances that may enter the

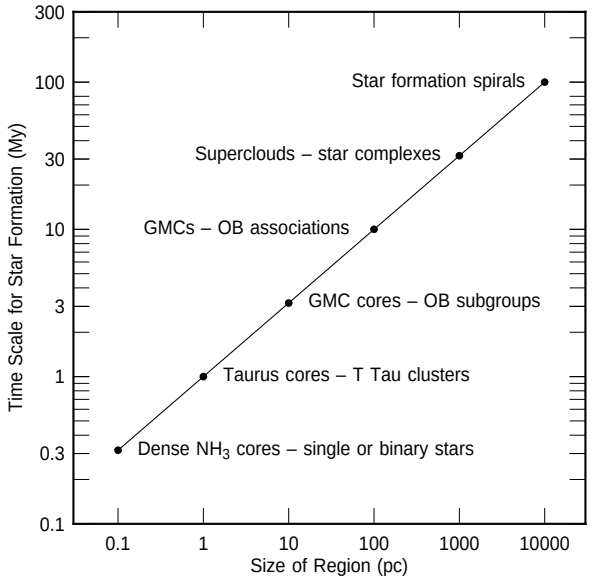

Figure 3. Schematic diagram showing how the duration of star formation in regions of various sizes increases with the square root of the size.

cloud, from an initial non-uniformity in the pre-cloud gas, for example, or from a galactic gradient, will not smooth out much before star formation actually begins. That is, *there is not much time for mixing before star formation.* Indeed, the dominant mode of star formation in galaxy disks involves giant cloud complexes that are likely to be initially inhomogeneous in elemental distribution at a level of perhaps ± 0.05 dex. The stars that form in these clouds should be equally inhomogeneous.

3. Mixing of Supernova Debris During Star Formation

Hierarchical structure in star-forming regions implies that star formation is concentrated into a small fraction of the volume, and the ensuing supernova contamination is localized. For fractal clouds, the volume filling factor of dense gas is

$$f_{\rm dense\ gas} = \text{peak density contrast}^{(D/3)-1} \sim 0.1 \tag{1}$$

for fractal dimension $D = 2.3$ (Elmegreen & Falgarone 1996) and peak density contrast of $\sim 10^4$. Thus, in any region, star formation occurs in only 10% of the volume.

The typical size of a supernova remnant in a region of star formation is only $\sim 10 - 50$ pc. From Cioffi, McKee & Bertschinger (1988) the final size of a remnant following the pressure-driven snowplow phase is

$$R_{final} = 4.93 R_{PDS} \left(\frac{E_{51}^{1/14} n_0^{1/7}}{a_{10}} \right)^{3/7} \tag{2}$$

where

$$R_{PDS}(pc) = 14.0 \left(\frac{E_{51}^{2/7}}{n_0^{3/7}} \right). \quad (3)$$

Here E_{51} is the supernova energy, n_0 is the preshock density, and a_{10} is the preshock velocity dispersion in units of 10 km s^{-1}. Thus

$$R_{final}(pc) = 69 E_{51}^{0.32} n_0^{-0.37} a_{10}^{-0.43}. \quad (4)$$

But $a(km\ s^{-1}) \sim 0.7 S(pc)^{1/2}$ from the molecular cloud correlations, and $n_0 \sim 5000 S(pc)^{-1}$ for pressure $\rho a^2 \sim 4 \times 10^5$ k$_B$ in a star-forming region. Then we get

$$R_{final}(pc) \sim 10 E_{51}^{0.32} S(pc)^{0.15}, \quad (5)$$

which is relatively insensitive to scale. If the supernova occurs in a region that is cleared of gas by previous HII regions and wind pressures, then it can become larger than this.

The size of a region of star formation in which OB stars form is typically larger than the size of a supernova remnant in such a region. There *is* a characteristic (or minimum) size for such OB star-forming regions even though there is no characteristic size for star-forming regions in general. This is because it takes a minimum number of $\sim 10^4$ stars before an O-type star is likely to form at all under a random sampling of the initial stellar mass function. Thus low mass clouds tend to form only low mass stars (because these stars are common) and high mass clouds tend to form OB stars in addition to low mass stars. The star-forming regions in which supernovae are likely to occur span a distance scale greater than $\sim$ 10 pc, possibly even greater than $\sim$ 100 pc, as suggested also by the plotted points for OB subgroups and associations in figure 2. These scales are comparable to or larger than the associated supernova remnant sizes, so *supernova contamination in a region of star formation should be spotty and localized*. The supernova debris will therefore mix with only part of the star-forming gas, and may even get highly concentrated in several small regions if the explosion happens to occur at close range to the cloud. Note that R_{final} in the above equation is small, so according to this, a lot of contamination will be at a range less than $\sim$ 10 pc.

Debris from multiple supernovae in an OB association should contaminate a few dense clouds and leave the rest in a shadow or far away. Thus *the clumpy, hierarchical nature of star-forming regions should lead to abundance inhomogeneities during the star formation/supernova epoch*, which is a $3 - 20$ My year period following the onset of star formation in a region where OB stars form. Studies of supernova remnants in regions of star formation were made by Junkes et al. (1992) and others.

4. Penetration of Supernova Debris into a Shocked Cloud

In a simple bow shock, there is a contact discontinuity between the dense cloud and the SN gas, and this surface has no direct mixing in equilibrium conditions. Kelvin-Helmholtz and Rayleigh-Taylor instabilities on this surface will mix the gas, however, and these instabilities should be responsible for contamination of

the cloud by supernova material. In numerical simulations of this process, such mixing is invariable *behind the cloud*, and not in the cloud core (e.g., Xu & Stone 1995).

It is unknown if SN debris also mixes with the gas in a compressed cloud core. Stone & Norman (1992) simulate a shock/cloud collision with $\gamma = 5/3$ and suggest that a Richtmyer-Meshkov instability might lead to mixing at the front surface and inside the core. Foster & Boss (1996, 1997) consider a shock/cloud collision with $\gamma = 1$ and get a very thin region between the cloud and the shock in the SN ejecta. This thin region allows Rayleigh-Taylor fingers at the head of the cloud to penetrate into the core and aid mixing with dense, pre-star-formation material.

Supernova interactions with fractal or hierarchically structured clouds have not yet been modeled.

5. Mixing of SN-contaminated Clouds after SF

The size-linewidth-time relation in a hierarchical cloud implies that many small regions of SF come and go before the large region is finished. This is also evident from the schematic diagram in figure 3. One implication of this is that the large star-forming clouds, which cannot be easily destroyed by internal star formation, probably move around and get recycled as even larger scales in the hierarchy continue to form stars. In this case, GMC's can have several epochs of supernova contamination, and each one can increase the dispersion of the final stellar abundances in a stochastic fashion before all star formation stops in the region.

An example is offered by the formation in the Solar neighborhood. Most of it began 30-50 My ago when the neighborhood was shocked by the local spiral arm, which is now the Carina arm. This assumes a pattern speed for the Galactic spiral system of 13.5 km s^{-1} kpc^{-1} from Yuan (1969). The first generation of star formation probably made the Cas-Tau association (Blaauw 1984), in addition to some clusters, such as ζ Sculptoris and the Pleiades. This first generation also could have caused the expansion of Lindblad's ring, which now seems to contain the Orion, Perseus, and Sco-Cen OB associations along the periphery (see review in Pöppel 1997). The Cas-Tau association at the center of this ring now has very little gas, so presumably its residual gas and other spiral arm gas got collected into Lindblad's ring, and eventually into the local associations. Thus the current supernova contamination of Orion and other local clouds is probably the second time this has happened since the spiral wave passed by.

The tilt of Gould's Belt has been attributed to the impact of an extra-galactic cloud (Franco et al. 1988; Comerón & Torra 1993), but there are other explanations such as a Parker instability (Gomez de Castro & Pudritz 1992; Shibata & Matsumoto 1991), and general perturbations from the LMC (Edelsohn & Elmegreen 1997). Maybe the spiral arm itself is responsible for the tilt. The shock in a spiral arm contains more than enough speed to elevate the gas to one scale height; any asymmetry in the spiral potential relative to the gas midplane could conceivable lead to a tilted gas distribution when giant clouds form.

The primary disadvantages of the cloud impact model are (1) that the local star formation seemed to begin just when the local region was at or near the

crest of a spiral arm, and such timing for an impact would be unlikely, and (2) that corrugations like this are common in the spiral arms of the inner galaxy (Pandey, Bhatt, & Mhara 1988; Sanders, Solomon, & Scoville 1984) and other galaxies (Florido et al. 1991), and it is unlikely all were formed by cloud impacts. Nevertheless, the impact model is intriguing from the point of view of abundance anomalies in Orion and other local regions, because an impacting high velocity cloud could have contaminated the disk with low metallicity material (Cunha & Lambert 1992; Edvardsson et al. 1995).

6. Mixing of SN-contaminated Cloud Debris after SF

Ultimately the star-forming gas gets converted to low density by ionization, heating, and evaporation. These processes cause *atomic level* mixing.

The large-scale star-forming regions are also stretched by increased shear and tidal forces when they enter the interarm. These processes cause *cloud-to-cloud* mixing rather than atom-to-atom mixing, but they also expose the dense gas to stray stellar enegy which can lead to more ionization, heating, and evaporation. It follows that *passing from an arm to the interarm region should help homogenize the gas at both the cloud and the atomic level.*

In the inner part of the Milky Way, the next spiral density wave arm arrives rather quickly, in only 50 My years or less. This is before cloud destruction is complete so there is a significant amount of dense molecular gas and star formation still in the interarm. For example, figure 1 shows a lot more gas and dense knotty emission in the interarm region at small radii than large radii.

Based on such analyses, one might expect cloud self-destruction to be more complete in the interarm regions in the outer part of the Milky Way than the inner part. This implies that the interarm homogenization of supernova enriched gas should change with radius, and so should the relative dispersion in abundances.

Post-star-formation mixing is also possible in chimney vents and giant bubbles that send enriched material into the halo where it can disperse over a radial range of perhaps a kiloparsec or more. In the hot gas, the supernova debris can mix atom-by-atom, so this form of dispersal is at the atomic level.

7. Conclusions

1. Pre-star formation clouds should be inhomogeneous as a result of their chaotic and large-scale formation processes.
2. Inhomogeneities should increase during star formation as a result of the clumpy, hierarchical structure of young stars. The penetration depth of SN debris into triggered clouds is unknown, however.
3. Short-time cloud recycling should continue to increase the metallicity and the metallicity dispersion until all star formation stops.
4. Ionization, heating, evaporation, and hot chimneys should homogenize the gas at the atomic level, while general galactic shear should mix at the cloud-to-cloud level.
5. Passing to an interarm region should disperse a cloud complex and aid the homogenization process by allowing deeper penetration of background radiation.

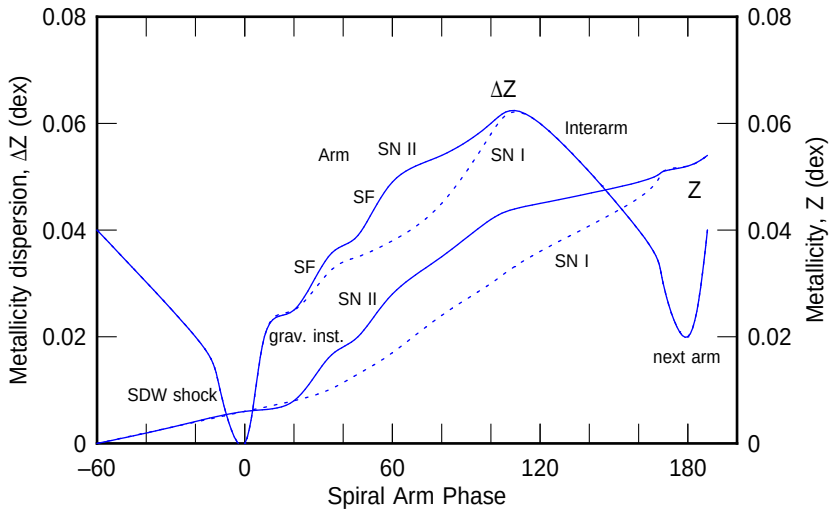

Figure 4. Schematic diagram of the change with spiral arm phase of the elemental abundance and the dispersion in the elemental abundance, based on the qualitative model presented in the text. Features related to star formation (SF), spiral arms and interarms, spiral density wave (SDW) shocks, and supernovae (SN) are shown.

A schematic diagram of the progressive change in abundance and abundance dispersion with phase in a spiral density wave is shown in figure 4. The contaminations from Type I and Type II supernova debris are tracked separately, because only the Type II debris (e.g., Oxygen) correlates with star formation. The Type I debris (e.g. Iron) is added more continuously to the gas as the comoving old stars evolve into supernovae. The vertical scales on the left and right are pure conjecture, but they sensibly follow from the discussion given above.

References

Blaauw, A. 1984, Irish AJ, 16, 141

Block, D.L., Elmegreen, B.G., Stockton, A., & Sauvage, M. 1997, ApJ, 486, L95

Cioffi, D.F., McKee, C.F. & Bertschinger, E. 1988, ApJ, 334, 252

Cohen, R.S., Dame, T.M., Garay, G., Montani, J., Rubio, M., & Thaddeus, P. 1988, ApJ, 331, L95

Comerón, F., & Torra, J. 1993, A&A, 281, 35

Cunha, K., & Lambert, D.L. 1992, ApJ, 399, 586

Dame, T., Elmegreen, B.G., Cohen, R., & Thaddeus, P. 1986, ApJ, 305, 892

Edelsohn, D. & Elmegreen, 1997, MNRAS, 287, 947

Edvardsson, B., Pettersson, B., Kharrazi, M., & Westerlund, B. 1995, A&A, 293, 75

Elmegreen, B.G. 1994, ApJ, 433, 39

Elmegreen, B.G., & Elmegreen, D.M. 1987, ApJ, 320, 182

Elmegreen, B.G., & Falgarone, E. 1996, ApJ, 471, 816

Elmegreen, B.G., & Efremov, Y.N. 1996, ApJ, 466, 802

Falgarone, E., Puget, J.L., & Pérault, M. 1992, A&A, 257, 715

Florido, E., Battaner, E., Sanchez-Saavedra, M.L., Prieto, M., & Madiavilla, E. 1991, MNRAS, 251, 193

Foster, P.N., & Boss, A.P. 1996, ApJ, 468, 784

Foster, P.N., & Boss, A.P. 1997, ApJ, 489, 346

Franco, J., Tenorio-Tagle, G., Bodenheimer, P., Mözyczka, M., & Mirabel, I.F. 1988, ApJ, 333, 826

Gomez de Castro, A., & Pudritz, R.E. 1992, ApJ, 395, 501

Grabelsky, D.A., Cohen, R.S., May, J., Bronfman, L., Thaddeus, P. 1987, ApJ, 315, 122

Hunter, D.A. 1997, Rev.Mex.AA (Conf.Ser.), 3, 1

Junkes, N., Fürst, E., & Reich, W. 1992, A&A, 96, 1

Knapen, J.H., Cepa, J., Beckman, J.E., Soledad Del Rio, M., & Pedlar, A. 1993, ApJ, 416, 563

Lada, C.J., Margulis, M., Sofue, Y., Nakai, N., & Handa, T. 1988, ApJ, 328, 143

Lemme, C., Walmsley, C.M., Wilson, T.L., & Muders, D. 1995, A&A, 302, 509

Loren, R.B. 1989, ApJ, 338, 902

Pandey, A.K., Bhatt, B.C., & Mahra, H.S. 1988, A&A, 189, 66

Pöppel, W. 1997, Fundam.Cosmic Phys., 18, 1

Rand, R.J., & Kulkarni, S.R. 1990, ApJ, 349, L43

Sanders, D.B., Solomon, P.M., & Scoville, N.Z. 1984, ApJ, 276, 182

Shibata, K., & Matsumoto, R. 1991, Nature, 353, 633

Solomon, P.M., Rivolo, A.R., Barrett, J., & Yahil, A. 1987, ApJ, 319, 730

Stone, J.M., & Norman, M.L. 1992, ApJ, 390, L17

Stutzki, J., & Güsten, R. 1990, ApJ, 356, 513

Thornley, M.D., & Mundy, L.G. 1997a, ApJ, 484, 202

Thornley, M.D., & Mundy, L.G. 1997b, ApJ, 490, 682

Williams, J.P., de Geus, E.J., & Blitz, L. 1994, ApJ, 428, 693

Xu, J. & Stone, J.M. 1995, ApJ, 454, 172

Yuan, C. 1969, ApJ, 158, 889